Reaction-Diffusion Media with Excitable Oregonators Coupled by Memristors

Xiyuan Gong, Tetsuya Asai and Masato Motomura
Graduate School of Information Science and Technology, Hokkaido University
Kita 14, Nishi 9, Kita-ku, Sapporo 060–0814, Japan
Phone: +81-11-706-6080, Fax: +81-11-706-7890
Email: xiyuan@lalsie.ist.hokudai.ac.jp, {asai, motomura}@ist.hokudai.ac.jp

***Abstract*— We numerically investigated the dynamics of a new reaction-diffusion-type excitable medium where the diffusion coefficient is represented by *memristive* dynamics. This type of a medium consists of an array of excitable Oregonators, and each Oregonator is locally coupled with other Oregonators via *memristors*, which were claimed to be the fourth circuit element exhibiting a relationship between flux ϕ and charge q. Through extensive numerical simulations, we found that the memristor conductances were modulated by the excitable waves and controlled the velocity of the waves, depending on the memristor's polarity. Further, different nonuniform spatial patterns were generated depending on the initial condition of Oregonator's state, memristor polarity and stimulation.**

I. Introduction

Semiconductor reaction-diffusion (RD) computing large-scale integrations (LSIs) implementing RD dynamics have been proposed in the literature [3]. These LSIs were mostly designed by digital, analog, or mixed-signal complementary-metal-oxide-semiconductor (CMOS) circuits of cellular neural networks (CNNs) or cellular automata (CA). Electrical cell circuits were designed to implement several CA and CNN models of RD systems [4], [5], [6], [7], [8], as well as fundamental RD equations [9], [10], [11], [12]. Each cell is arranged on a two-dimensional (2-D) square or a hexagonal grid and is connected to adjacent cells through coupling devices that transmit the cell's state to its neighboring cells, as in conventional CAs. For instance, an analog-digital hybrid RD chip [5] was designed for emulating a conventional CA model for Belousov-Zhabotinsky (BZ) reactions [13]. A full-digital RD processor [6] was also designed on the basis of a multiple-valued CA model, called *excitable lattices* [14]. An analog cell circuit was also designed to be equivalent to spatial-discrete Turing RD systems [10]. A full-analog RD chip that emulates BZ reactions has also been designed and fabricated [9].

Blueprints of non-CMOS RD chips have been designed, for example, a single-electron RD device [15]. The authors previously proposed an RD device based on minority-carrier transport in semiconductor devices [16]. The point of our idea was to simulate chemical diffusion with minority-carrier diffusion in semiconductors and autocatalytic chemical reactions with carrier multiplication in *p-n-p-n* negative resistance diodes. Using CMOS and non-CMOS RD circuits enables us to simulate a variety of autocatalytic reactions and open up a variety of application fields for RD devices.

In this study, we attempt to reclaim a new field of semiconductor RD LSIs and propose a new RD-based excitable medium, keeping in mind the hardware implementation. Recently, the so-called "memristors," originally introduced by Leon Chua in 1971 [2] and claimed to be the fourth circuit element exhibiting a relationship between flux ϕ and charge q, have again been in the spotlight since Strukov *et al.* presented equivalent physical examples [17]. Although the presented device was a bipolar resistive RAM that did not "directly" exhibit a relationship between ϕ and q, the device behaved as a non-volatile resistor whose resistance was continuously controlled by the amount of the charge flow (current). Here, the following question arises: What happens if one replaces resistors for diffusion in analog RD LSIs with memristors? This is the primary purpose of this investigation in this work. Through extensive numerical simulations, we found that i) the memristor's conductances were modulated by excitable waves propagating on the memristor, depending on the memristor's polarity; ii) velocity of the excitable wave propagation is thus modulated by the change of memristor conductance, and the degree of the modulation is inversely proportional to the time constant of the memristor's model, and iii) different and interesting nonuniform spatial patterns were generated depending on the initial condition of Oregonator's state, memristor polarity and stimulation. In the following sections, we introduce an excitable RD model with memristors and show the spatiotemporal behaviors of 1-D and 2-D RD models through extensive numerical simulations.

II. The Model

A general model of memristors is explained in terms of *memristance* $M(q)$ [2]; however, we here use a comprehensive model represented by

$$i = g(w)v, \quad \frac{dw}{dt} = i \tag{1}$$

where v represents the voltage across the memristor; i, the current of the memristor; w, the nominal internal state of the memristor and corresponds to the charge flow of the memristor, and $g(w)$, the monotonically increasing function with increasing w [17]. This model implies that positive (or negative) i (current flow) increases (or decreases) w, which results in an increase (or decrease) in the memristor conductance $g(w)$. Figure 1 illustrates these aspects of memristors,

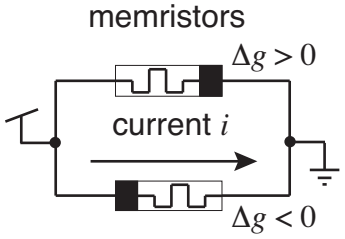

Fig. 1. Memristor symbols and polarity definition

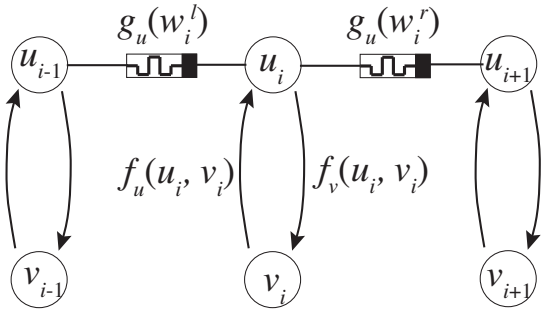

Fig. 2. Electrical representation of RD system whose diffusive resistors are replaced with memristors

where Δg corresponds to dw/dt and hence $dg(w)/dt$. In what follows, we integrate these dynamics into a general RD model.

A 1-D reaction-diffusion system is described by

$$\frac{\partial u(x)}{\partial t} = g_u \nabla^2 u(x) + f_u[u(x), v(x)] \quad (2)$$

$$\frac{\partial v(x)}{\partial t} = g_v \nabla^2 v(x) + f_v[u(x), v(x)] \quad (3)$$

where $u(x)$ and $v(x)$ denote the concentrations of two different chemical species at spatial position x; $g_{u,v}$, the diffusion coefficients; and $f_{u,v}(\cdot)$, the reaction model. Here, we employ Oregonators [1] for the reaction model; *i.e.*,

$$f_u[u(x), v(x)] = u(x)[1 - u(x)] - av(x)\frac{u(x) - b}{b + u(x)}$$

$$f_v[u(x), v(x)] = u(x) - v(x)$$

where a and b denote the reaction parameters. Depending on the reaction parameters, the Oregonator exhibits limit-cycle oscillations and excitatory behaviors. In this paper, we only consider the excitable properties ($g_v = 0$ only), which means the Oregonator is stable as long as an external stimulus is not applied. In the model, three types of reaction states are defined at one Oregonator, namely, inactive, active, and refractory states. When the Oregonator is inactive, it is easily activated by an external stimulus, following which it changes to the refractory state. During the refractory state, the Oregonator cannot be activated even if an external stimulus is applied.

Although g_u is constant in general RD models, we are more interested in a system where g_u is locally modified by the potential gradient of $u(x)$.

When $u(x)$ and $v(x)$ are represented by voltages on the RD hardware, the gradient (diffusion terms in the RD model) is represented by linear resistors [9]. For example, if one discretizes Eq. (2) spatially as

$$\frac{du_i}{dt} = \frac{g_u \cdot (u_{i-1} - u_i) + g_u \cdot (u_{i+1} - u_i)}{\Delta x^2} + f_u(\cdot)$$

where i is the spatial index, and Δx the discrete step in space, terms $g_u \cdot (u_{i-1} - u_i)$ and $g_u \cdot (u_{i+1} - u_i)$ represent current flowing into the i-th node from the $(i-1)$-th and $(i+1)$-th nodes via two resistors whose conductance is represented by g_u. The spatial Laplacian ∇^2 in Eq. (2) can be approximated as

$$\nabla^2 u(x) = \frac{u_{i-1} + u_{i+1} - 2u_i}{\Delta x^2}.$$

Here, we introduce the memristor model described by Eq. (1); in this model, the resistors are replaced with memristors. The resulting point dynamics are given as

$$\frac{du_i}{dt} = \frac{g_u(w_i^l)(u_{i-1} - u_i) + g_u(w_i^r)(u_{i+1} - u_i)}{\Delta x^2} + f_u(\cdot)$$

$$\frac{dv_i}{dt} = f_v(\cdot)$$

where $g_u(\cdot)$ denotes the monotonically increasing function defined by

$$g_u(w_i^{l,r}) = g_{\min} + (g_{\max} - g_{\min}) \cdot \frac{1}{1 + e^{-\beta w_i^{l,r}}}$$

where β denotes the gain; $g_{\min}$ and $g\ _{max}$ denote the minimum and maximum coupling strengths, respectively, and $w_i^{l,r}$ denote the variables for determining the coupling strength of the i-th Oregonator (l: leftward, r: rightward). Finally, we introduce the following memristive dynamics for $w_i^{l,r}$:

$$\tau \frac{dw_i^{l,r}}{dt} = g_u(w_i^{l,r}) \cdot \eta_1 \cdot (u_{i-1,i+1} - u_i) \quad (4)$$

where the right-hand side represents the current of the memristors in Eq. (1), and η_1 denotes the polarity coefficient ($\eta_1 = +1 : w_i^l$, $\eta_1 = -1 : w_i^r$). The model above corresponds to an electrical RD system consisting of Oregonators whose diffusive resistors are replaced with memristors (Figure 2).

III. Simulation Results

In the following simulations, we use the following parameters for memristors: $\beta = 1$, $g_{\min} = 10^{-4}$, and $g_{\max} = 10^{-1}$.

A. 1-D Reaction-Diffusion Medium

First, we simulated the basic model shown in Figure 3(a). One side of the boundary was stimulated by a periodic pulse sequence, and the conductance of the memristor was measured. The initial conductance of the memristor was set at zero. Figure 3(c) shows the simulated results. The conductance was increased considerably during the onset of the input pulse, which resulted in a small increase in the conductance. We roughly estimated Δg per single pulse (0.17 mS/pulse). Figure 3(b) shows the opposite simulation setup. In this simulation, the polarity of the memristor was inverted; therefore, one can expect the conductance to be decreased by the input pulses. The initial conductance was chosen such that stimulations

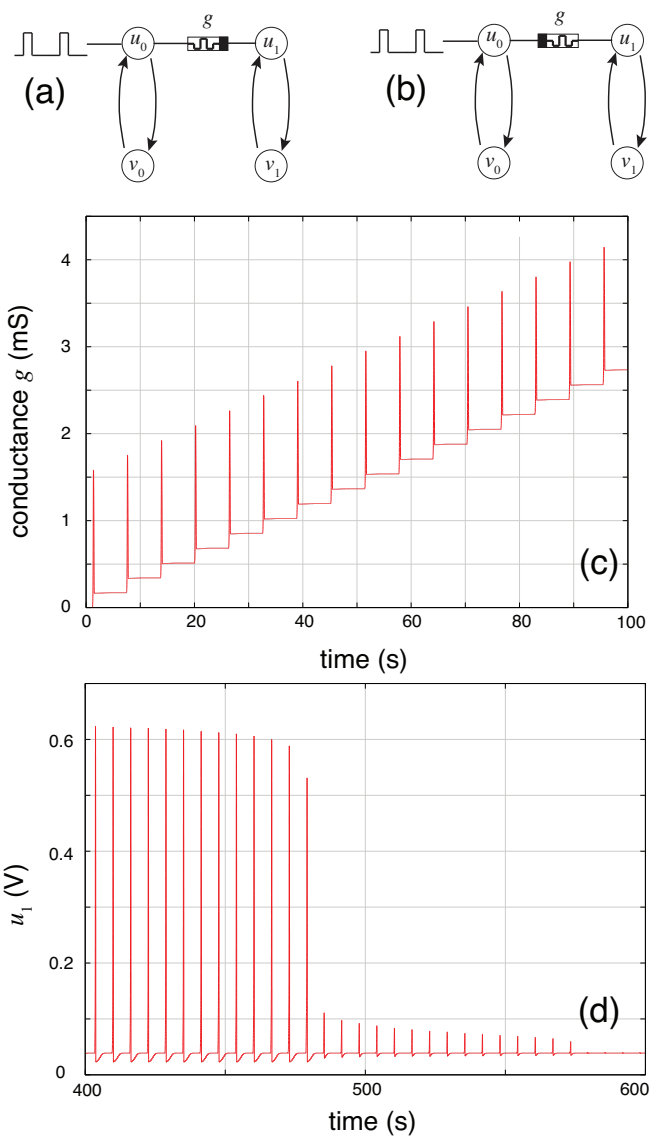

Fig. 3. Simulation results for two Oregonators with memristors

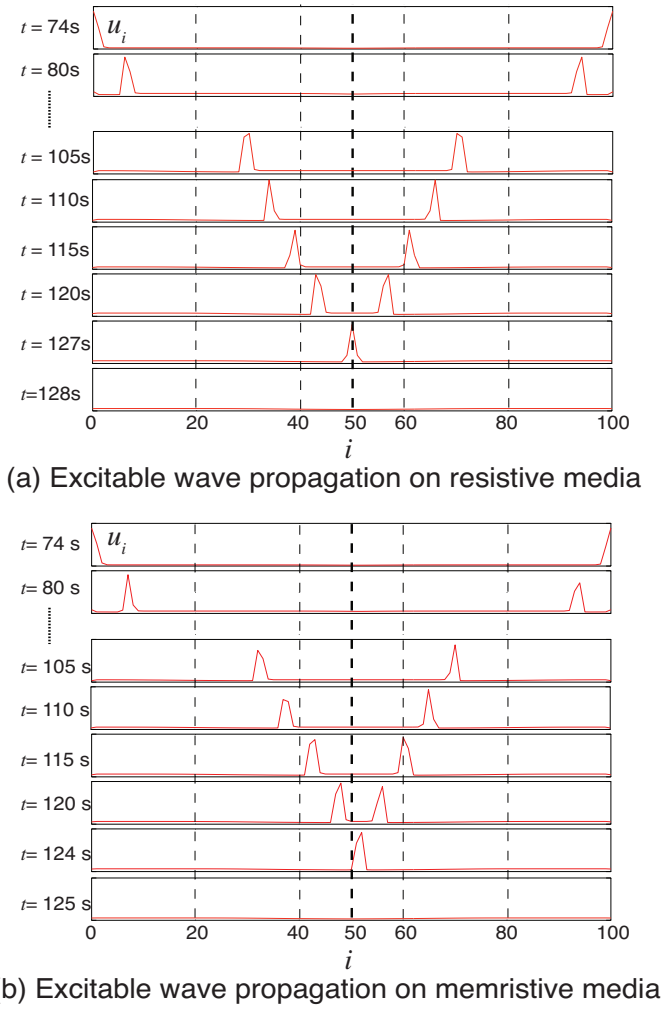

Fig. 4. Simulation results for 100 Oregonators consisting of normal resistors (a) and memristors (b)

to u_0 could cause chain excitation on u_1 via the memristor. Figure 3(d) shows the temporal responses of u_1. The stimulus was initially applied (u_1 was excited), but was terminated because of the decrease in the conductance. It should be noted that in both models of Figures 3(a) and (b), the boundary condition is Neumann boundary condition.

Figure 4(a) shows the simulation results of a 1-D medium with 100 Oregonators without memristive effects. Excitable wave propagation on the medium is apparent. Both boundaries were simultaneously stimulated, and the waves collided at the center position (following which they disappeared). When the memristive effects were introduced, given that the coupling strength $g_u(w_i^{l,r})$ is modified by the direction of wave propagation, the results were different from those shown in Figure 4(a). Figure 4(b) shows the simulation results of a 1-D medium consisting of 100 Oregonators with memristive effects, where the velocity of each excitable wave was different depending on the direction of wave propagation, which resulted in wave collision at a position other than the center (following which the waves disappeared). Excitable waves moving rightward (in the figure) increased $w_i^{l,r}$ of the memristors under the wave, whereas the leftward waves decreased $w_i^{l,r}$ under the wave, as a result of the polarity of memristors shown in Figure 1.

Then, we prepared a 1-D medium with 100 Oregonatorsm as well, and we assumed a cyclic boundary condition. After stimulating one node (the 58th node in our simulation), an excitable wave propagates on the medium in a cyclic-looping manner. In the initial stimulation, wave propagation was unidirectional because the refractory states of the Oregonators were controlled. The initial conductance of the memristors was set at g_{min}. Figure 5 shows the time courses of all the nodes (u_i) where the magnitudes are represented by gray-scale tones. Spatial (nonuniform) patterns developed over time. Surprisingly, the developed patterns were periodic, like Turing patterns, and they reached equilibrium at around 2×10^4 s.

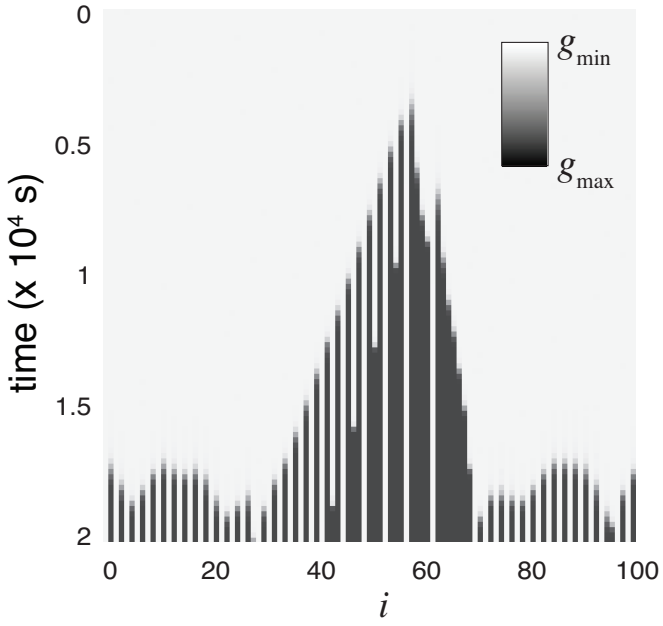

Fig. 5. Spatial pattern formation on 1-D excitable media with memristors under cyclic boundary condition

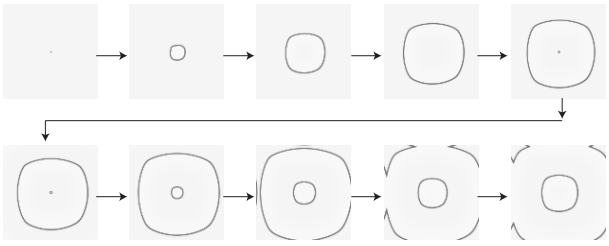

Fig. 6. Ocean-surface-wave patterns on 2-D media with memristors

B. 2-D Reaction-Diffusion Medium

Finally, we prepared a 2-D memristive medium with 100 × 100 Oregonators and assumed a cyclic boundary condition. For the 2-D RD medium, we introduce the following memristive dynamics for $w_i^{up,d}$:

$$\tau \frac{dw_i^{up,d}}{dt} = g_u(w_i^{up,d}) \cdot \eta_2 \cdot (u_{i-1,i+1} - u_i), \tag{5}$$

where $w_i^{up,d}$ denotes the variables for determining the coupling strength of the i-th Oregonator (up: upward, d: downward); and η_2, the polarity coefficient ($\eta_2 = +1 : w_i^{up}$, $\eta_2 = -1 : w_i^d$). We assumed both the polarity coefficients η_1 (Eq. (4)) and η_2 to be -1.

The initial state of all the Oregonators was set to be inactive state. After stimulating the center node, the excitable waves propagated outwards, resulting in the generation of patterns of ocean surface waves. Figure 6 shows the time courses of all the nodes ($u_{i,j}$) ($u_{i,j} = 0$: white, $u_{i,j} = 1$: black). The velocity of waves propagation was deferred depending on the direction of the wave propagation. According to the polarity of the memristors ($\eta_1, \eta_2 = -1$), the conductance of the memristors shown on the right-hand side and below would

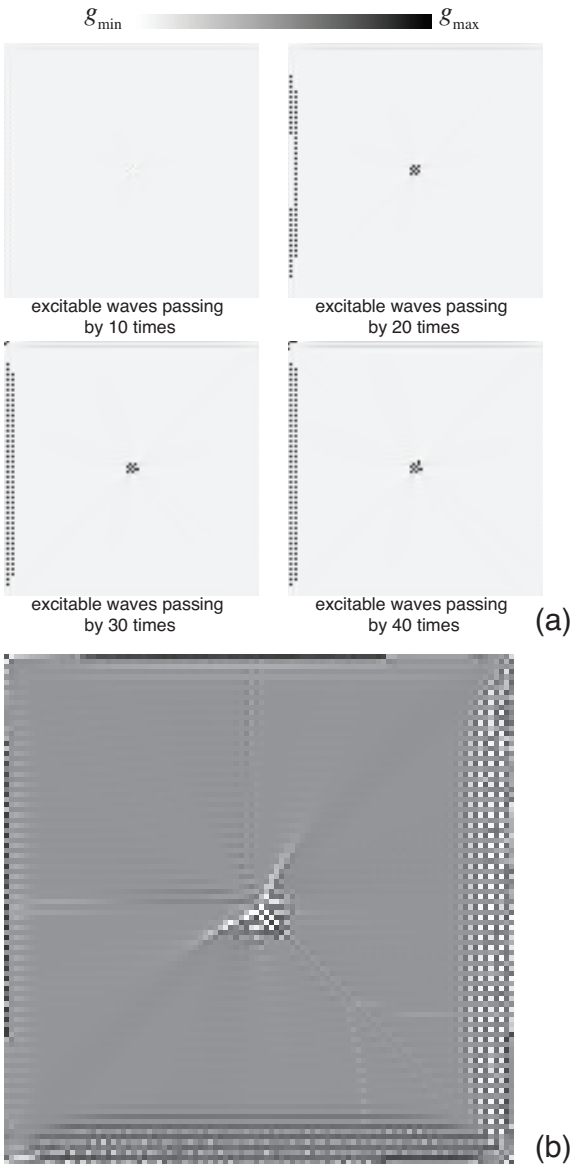

Fig. 7. Simulation results on conductance of memristors for 2-D media (ocean-surface-wave patterns)

increase whereas the conductance of those shown on the left-hand side or above would decrease; therefore, one can expect the waves to collide at the left-hand side and upward. Figure 7 shows the conductance of all the nodes, where the magnitudes are represented by gray-scale tones. It should be noted that these results were plotted when the conductance condition was stable given that the conductance changes considerably when the wave is propagating. Even after the waves propagated 10 times, the change in conductance was still small, after the waves propagated over that 20 times at the position where the waves generated at the beginning and collided, the memristor conductance changed considerably (Figure 7(a)). Figure 7(b) shows the conductance of all the nodes over a sufficient time period.

Then, instead of extraneous stimulus, the initial stimulation

Fig. 8. Clockwise and counterclockwise spiral patterns on 2-D media with memristors

was changed by controlling the states of the Oregonators. In Figure 8, the values of $u_{i,j}$ are represented on a gray scale ($u_{i,j} = 0$: white, $u_{i,j} = 1$: black). Several Oregonators next to the inactive Oregonators were initially set in a refractory state (down side of the black bar in the top-left snapshot in Figure 8). The inactive Oregonators next to the black bar were suppressed by the adjacent Oregonators in the refractory state (Oregonators in black bar). When the inactive Oregonators were in an active or inactive state, the wave rotated inwards, which resulted in the generation of clockwise and counterclockwise spiral patterns. Depending on the direction of wave propagation, the velocity of the rightward and downward waves was faster than that of the leftward and upward waves, given that η_1 in Eq. (5) and $\eta_2 = -1$ in Eq. (6) are both -1. Over time, the initial position of the generated waves, is moved to the lower right. Figure 9 shows the conductance of all the nodes, where the magnitudes are represented by gray-scale tones. It should be noted that these results were plotted when then conductance of some memristors was still unstable. Figure 8(b) shows the conductance of all the nodes over a sufficient time period.

IV. Summary

We proposed a new reaction-diffusion-based excitable medium that employed *memristors* to represent diffusion coupling. Through numerical simulations, we found that the medium could develop spatial patterns, and the memristor conductance changed according to the excitable wave collision and generation. We will further investigate the spatiotemporal properties of a model with random replacement (polarity) of memristors.

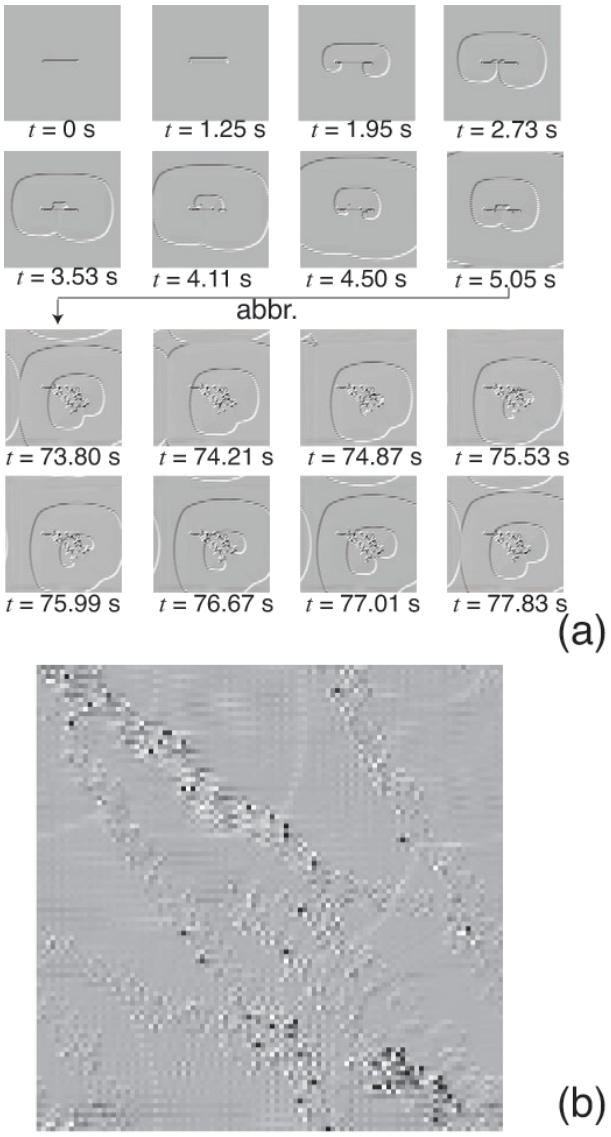

Fig. 9. Simulation results on conductance of memristors for 2-D media (clockwise and counterclockwise spiral patterns)

Acknowledgments

This study was supported by a Grant-in-Aid for Scientific Research on Innovative Areas [20111004] from the Ministry of Education, Culture, Sports, Science and Technology (MEXT) of Japan.

References

[1] http://www.scholarpedia.org/article/Oregonator
[2] Chua, L.O. [1971] "Memristor - the missing circuit element," *IEEE Trans. Circuit Theory* **18**(5), 507–519.
[3] Adamatzky, A., De Lacy Costello, B. & Asai T. [2005] *Reaction-Diffusion Computers* (Elsevier, London).
[4] Adamatzky, A., Arena, P., Basile, A., Carmona-Galán, R., De Lacy Costello, B., Fortuna, L., Frasca, M. & Rodríguez-Vázquez, A. [2004] "Reaction-diffusion navigation robot control: From chemical to VLSI analogic processors," *IEEE Trans. Circuit and Systems I* **51**(5), 926–938.

[5] Asai, T., Nishimiya, Y. & Amemiya, Y. [2002] "A CMOS reaction-diffusion circuit based on cellular-automaton processing emulating the Belousov-Zhabotinsky reaction," *IEICE Trans. Fundamentals* **E85-A**(9), 2093–2096.

[6] Matsubara, Y., Asai, T., Hirose, T. & Amemiya, Y. [2004] "Reaction-diffusion chip implementing excitable lattices with multiple-valued cellular automata," *IEICE Electronics Express* **1**(9) 248–252.

[7] Rekeczky, C., Roska, T., Carmona, R., Jiménez-Garrido, F. & Rodríguez-Vázquez, A. [2003] "Exploration of spatial-temporal dynamic phenomena in a 32 × 32-cell stored program two-layer CNN universal machine chip prototype," *J. Circuits, Systems and Computers* **12**(6), 691–710.

[8] Shi, B. E. & Luo, B. T. [2004] "Spatial pattern formation via reaction-diffusion dynamics in 32 × 32 × 4 CNN chip," *IEEE Trans. Circuit and Systems I* 51(5), 939–947.

[9] Asai, T., Kanazawa, Y., Hirose, T. & Amemiya, Y. [2005] "Analog reaction-diffusion chip imitating the Belousov-Zhabotinsky reaction with hardware Oregonator model," *Int. J. Unconventional Computing* **1**(2), 123–147.

[10] Daikoku, T., Asai, T. & Amemiya, Y. [2002] "An analog CMOS circuit implementing Turing's reaction-diffusion model," in *Proc. Int. Symp. Nonlinear Theory and Its Applications*, 809–812.

[11] Karahaliloglu, K. & Balkir, S. [2005] "Bio-inspired compact cell circuit for reaction-diffusion systems," *IEEE Trans. Circuit and Systems II*, **52**(9), 558–562.

[12] Serrano-Gotarredona, T. & Linares-Barranco, B. [2003] "Log-domain implementation of complex dynamics reaction-diffusion neural networks," *IEEE Trans. Neural Networks* **14**(5), 1337–1355.

[13] Gerhardt, M., Schuster, H. & Tyson, J. J. [1990] "A cellular automaton model of excitable media," *Physica D* **46**, 392–415.

[14] Adamatzky, A. [2001] *Computing in Nonlinear Media and Automata Collectives* (IoP Publishing, Bristol).

[15] Oya, T., Asai, T., Fukui, T. & Amemiya Y. [2005] "Reaction-diffusion systems consisting of single-electron circuits," *Int. J. Unconventional Computing* **1**(2), 177–194.

[16] Asai, T., Adamatzky, A. & Amemiya, Y. [2004] "Towards reaction-diffusion computing devices based on minority-carrier transport in semiconductors," *Chaos, Solitons & Fractals* **20**(4), 863–876.

[17] Strukov, D. B. Snider, G. S., Stewart, D. R. & Williams, R. S. [2008] "The missing memristor found," *Nature*, **452**(1), 80–83.